

Determination of two-photon exchange via e^+p/e^-p Scattering with CLAS12

Jan C. Bernauer · Volker D. Burkert · Ethan Cline · Axel Schmidt ·
Youri Sharabian

Received: date / Accepted: date

Abstract The proton elastic form factor ratio shows a discrepancy between measurements using the Rosenbluth technique in unpolarized beam and target experiments and measurements using polarization degrees of freedom. The proposed explanation of this discrepancy is uncorrected hard two-photon exchange (TPE), a type of radiative correction that is conventionally neglected. The effect size and agreement with theoretical predictions has been tested recently by three experiments. While the results support the existence of a small two-photon exchange effect, they cannot establish that theoretical treatments are valid. At larger momentum transfers, theory remains untested. This proposal aims to measure two-photon exchange over an extended and so far largely untested Q^2 and ε range with high precision using the CLAS12 experiment. Such data are crucial to clearly confirm or rule out TPE as the driver for the discrepancy as well as test several theoretical approaches, believed valid in different parts of the tested Q^2 range.

Keywords proton form factors · two-photon exchange

1 Introduction

Over more than half a century, proton elastic form factors have been extracted from electron-proton scatter-

ing experiments with unpolarized beams over a large range of four-momentum transfer squared, Q^2 , via the so-called Rosenbluth separation. The data indicate that the form factor ratio $\mu G_E/G_M$ is in agreement with scaling, i.e., that the ratio is close to 1. This ratio is also accessible via polarized beams with fundamentally different kinematics, and, especially at large Q^2 , improved precision. In contrast to the unpolarized result, the data indicate a roughly linear fall-off of the ratio. Some results of the different experimental methods, as well as recent fits, are compiled in Fig. 1. The two data sets are clearly inconsistent with each other, indicating that one method (or both) are failing to extract the proton's true form factor ratio. The resolution of this “form factor ratio puzzle” is crucial to advance our knowledge of the proton form factors.

The differences observed by the two methods have been attributed to two-photon exchange (TPE) effects [1–4], poised to affect especially the Rosenbluth method data. Two-photon exchange corresponds to the group of diagrams in the second order Born approximation of lepton scattering where two photon lines connect the lepton and proton. The case where one of these photons has negligible moment, the so-called “soft” case, is included in the standard radiative corrections, like Ref. [5,6]. The “hard” part, where both photons can carry considerable momentum, however, is not, but has been the focus of ongoing theoretical work.

To evaluate the theoretical prescriptions and test if TPE is indeed the solution of the puzzle, precise measurements over a wide Q^2 range are required. The most straightforward access to TPE is via measurement of the ratio of elastic e^+p/e^-p scattering,

$$R_{2\gamma} = \frac{\sigma_{e^+}}{\sigma_{e^-}} \approx 1 + 2\delta_{TPE}, \quad (1)$$

Jan C. Bernauer · Ethan Cline
Center for Frontiers in Nuclear Science, Stony Brook University, Stony Brook, NY, USA

Jan C. Bernauer
Riken BNL Research Center, Upton, NY, USA

Volker Burkert · Youri Sharabian
Thomas Jefferson National Accelerator Facility, Newport News, Virginia, USA

Axel Schmidt
The George Washington University, Washington, DC, USA

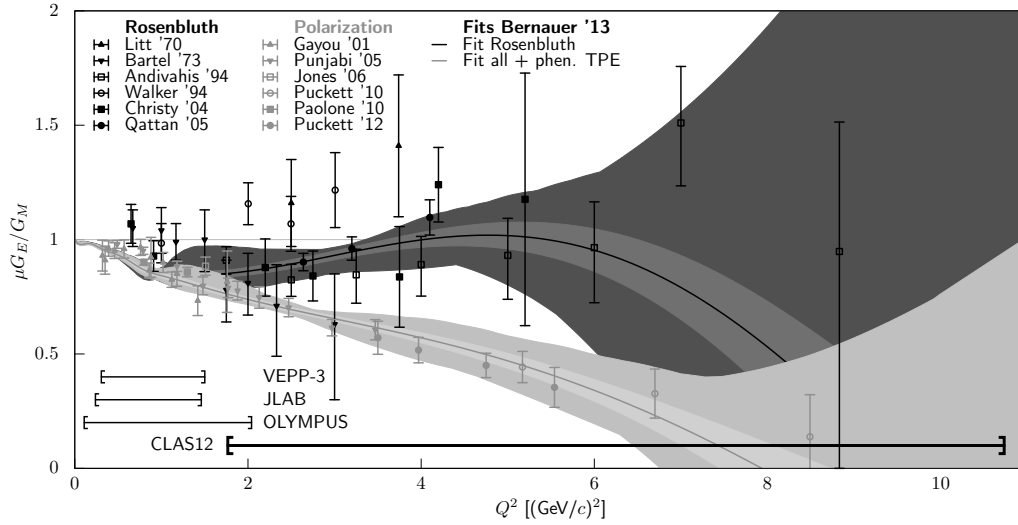


Fig. 1 The proton form factor ratio $\mu G_E/G_M$, as determined via Rosenbluth-type (black points, from [7–12]) and polarization-type (gray points, from [13–18]) experiments. While the former indicate a ratio close to 1, the latter show a distinct linear fall-off. Curves are from a phenomenological fit [19], to either the Rosenbluth-type world data set alone (dark curves) or to all data, then including a phenomenological two-photon-exchange model. We also indicate the coverage of earlier experiments as well as of the experiment described below.

here, δ_{TPE} is the correction to the Born level cross section introduced by TPE.

We propose a new definitive measurement of the TPE effect that would be possible with a positron source at CEBAF. By alternately scattering positron and electron beams from a liquid hydrogen target and detecting the scattered lepton and recoiling proton in coincidence with the large acceptance CLAS-12 spectrometer, the magnitude of the TPE contribution between Q^2 values of 2 and 10 GeV^2 could be significantly constrained. With such a measurement, the question of whether or not TPE is at the heart of the “proton form factor puzzle” could be answered definitively.

1.1 Previous work

One significant challenge is that hard TPE cannot be calculated in a model-independent way. There are several model-dependent approaches. A full description of the available theoretical calculations are outside of the scope of this letter. Suffice it to say that they can be roughly divided into two groups: hadronic calculations, e.g. [20], which should be valid for Q^2 from 0 up to a couple of GeV^2 , and GPDs based calculations, e.g. [21]. The latter give a good description of nucleon form factors and wide-angle Compton scattering at JLAB kinematics and should become valid for $Q^2 > 1$, where the early onset of scaling is observed in DIS. At these scales, point-like quarks start to be resolved and the emissions of quarks from and re-absorption into a nucleon are described by GPDs, the overlap of light cone

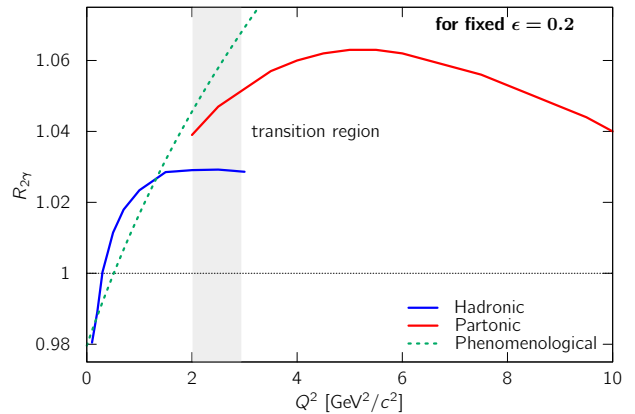


Fig. 2 A comparison of three classes of model-dependent predictions for $R_{2\gamma}$, shown as function of Q^2 for fixed $\epsilon = 0.2$. The hadronic prediction is the $N + \Delta$ calculation from Ref. [20]. The partonic prediction is the Gaussian GPD model from Ref. [21]. The phenomenological prediction comes from Ref. [19], and is shown in many of the figures that follow. The validity of hadronic approaches diminishes at higher Q^2 , while the validity of partonic approaches diminishes when Q^2 is small. Between $2 \lesssim Q^2 \lesssim 3 \text{ GeV}^2/c^2$, it would be natural to expect some transition between the two approaches.

wave functions. A comparison of examples of these two approaches is shown in Fig. 2.

Three contemporary experiments measured the size of TPE, based at VEPP-3 [22], Jefferson Lab (CLAS, [23–25]) and DESY (OLYMPUS, [26]). These experiments measured the ratio of positron-proton to electron-proton elastic cross sections. The kinematic reach of the three experiments is shown in Fig. 3. The kine-

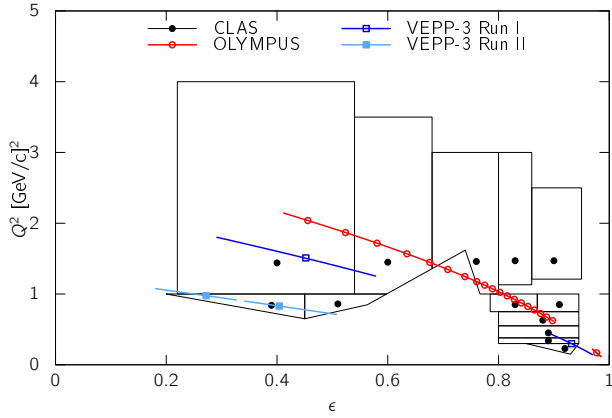


Fig. 3 Kinematics covered by the three recent experiments to measure the two-photon exchange contribution to the elastic ep cross section. The beam energy in the CLAS experiment was not fixed. The black polygons signify the phase space of data projected to the black (round) points.

matic coverage in these experiments is limited to $Q^2 < 2 \text{ GeV}^2$, and $\epsilon > 0.5$, where the two-photon effects are expected to be small, and systematics of the measurements must be extremely well controlled. Comparisons of the data with theoretical predictions find overall poor agreement, an indication that TPE is not fully understood from theory. Compared to phenomenological predictions [19], the agreement is good, indicating that TPE can indeed explain the majority of the discrepancy at the tested kinematics. However, at the highest Q^2 points, the predictions over-shoot the data considerably, pointing towards the possibility that TPE might not sufficiently explain the discrepancy at higher Q^2 .

We refer to [4] for a more in-depth review. The uncertainty in the resolution of the ratio puzzle jeopardizes the extraction of reliable form factor information, especially at high Q^2 , as covered by the Jefferson Lab 12 GeV program. Clearly, new data are needed.

2 Proposed experiment

Theories and phenomenological extractions predict a roughly proportional relationship of the TPE effect with $1 - \epsilon$ and a sub-linear increase with Q^2 . However, interaction rates drop sharply with smaller ϵ and higher Q^2 , corresponding to higher beam energies and larger electron scattering angles. This puts the interesting kinematic region out of reach for storage-ring experiments, and handicaps external beam experiments with classic spectrometers with comparatively small acceptance.

With the large acceptance of CLAS12, combined with an almost ideal coverage of the kinematics, measurements of TPE across a wide kinematic range are possible, complementing the precision form factor program

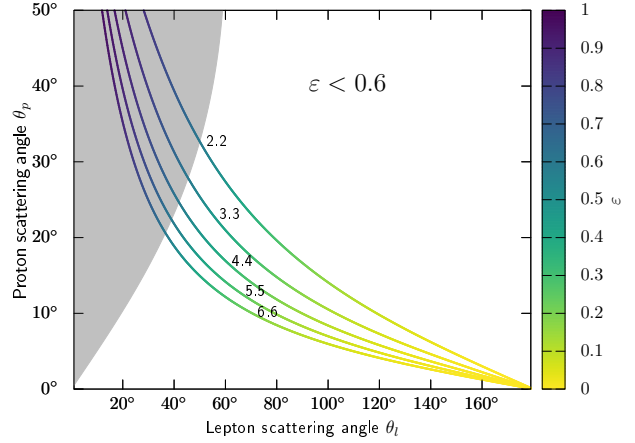


Fig. 4 Polar angle correlation and ϵ coverage for lepton and proton. Each line represents a different beam energy. For the shaded area, $\epsilon > 0.6$.

of Jefferson Lab, and testing both hadronic (valid at the low Q^2 end) as well as GPD-based (valid at the high Q^2 -end) theoretical approaches. Figure 4 shows the angle correlation between the lepton and the proton for different beam momenta. There is a one-to-one correlation between the lepton scattering angle and the proton recoil angle. For the kinematics of interest, say $\epsilon < 0.6$ and $Q^2 > 2 \text{ GeV}^2$ for the chosen beam energies from 2.2 to 6.6 GeV, nearly all of the lepton scattering angles falls into a polar angle range from 40° to 125° , and corresponding to the proton polar angle range from 8° to 35° . These kinematics are most suitable for accessing the TPE contributions. The setup will also be able to measure the reversed kinematics with the electrons at forward angle and the protons at large polar angles, i.e. the standard CLAS12 configuration of DVCS and most other experiments. While the two-photon exchange is expected to be small in this range, the sign change in TPE seen in the experiments, but not predicted by current theories, can be studied.

Figure 5 shows the expected elastic scattering rates covering the ranges of highest interest, with $\epsilon < 0.6$ and $Q^2 = 2 - 10 \text{ GeV}^2$. Sufficiently high statistics can be achieved within 10 hrs for the lowest energy and within 1000 hrs for the highest energy, to cover the full range in kinematics. Note that all kinematic bins will be measured simultaneously at a given energy, and the shown rates are for the individual bins in (Q^2, ϵ) phase-space. In order to achieve the desired kinematics reach in Q^2 and ϵ the CLAS12 detection system has to be used with reversed detection capabilities for leptons. The main modification will involve replacing the current Central Neutron Detector with a central electromagnetic calorimeter (CEC), a concept that has already

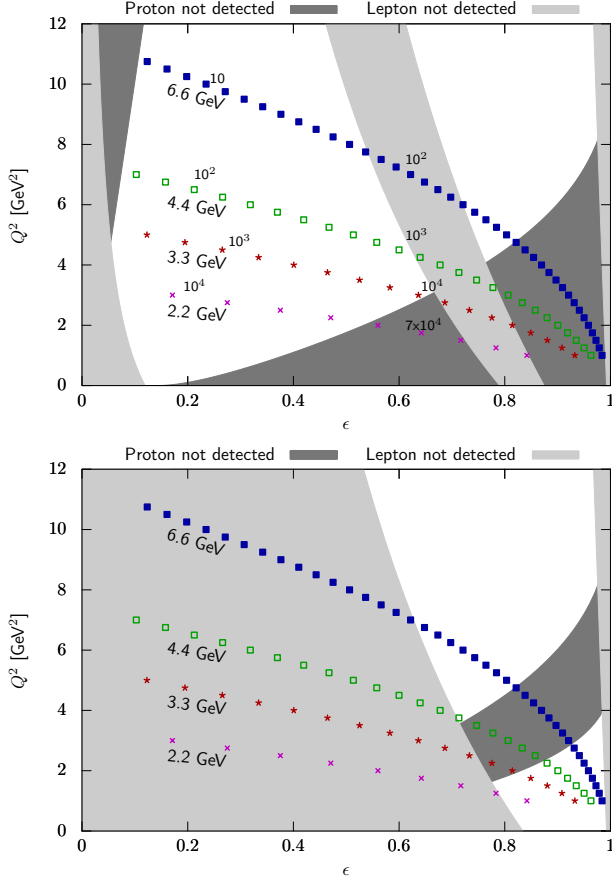


Fig. 5 Proposed kinematics for energies 2.2, 3.3, 4.4, 6.6 GeV in the $\epsilon - Q^2$ plane. Shaded areas are excluded by the detector acceptance. Top: proposed experiment; Bottom: standard setup. The numbers in the top plot indicate expected counts per hour.

been studied for the CLAS12 program. The CEC will not need very good resolution, which is provided by the tracking detectors, but will only be used for trigger purposes and for electron/pion separation. The strict kinematic correlation of the scattered electron and the recoil proton will be sufficient to select the elastic events. The CLAS12 configuration suitable for this experiment is shown in Fig. 6.

2.1 Central Electromagnetic Calorimeter

The Central Electromagnetic Calorimeter (CEC) will be used for trigger purposes to detect electrons elastically scattered under large angles and for the separation of electrons (positrons) and charged pions. The CEC will be a new detector for CLAS12, but based on a mature design from the original CLAS12 concept. The detector will use a novel tungsten powder/scintillating fiber calorimetry technology first proposed in 1999. This

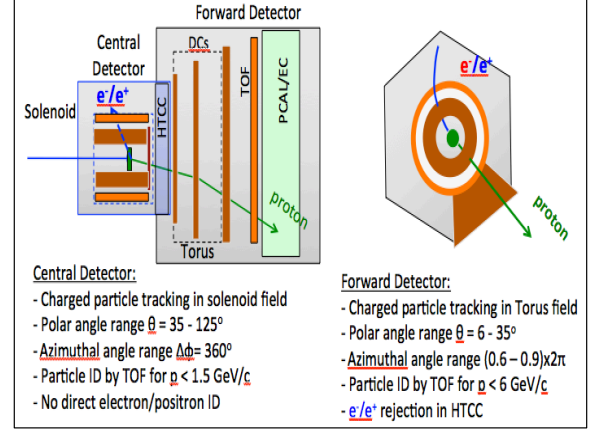


Fig. 6 CLAS12 configuration for the elastic e^-p/e^+p scattering experiment. The central detector will detect the electron/positrons, and the bending in the solenoid magnetic field will be identical for the same kinematics. The proton will be detected in the forward detector part. The torus field direction will be the same in both cases. The deflection in ϕ due to the solenoid fringe field will be of same in magnitude of $\Delta\phi$ but opposite in direction. The systematic of this shift can be controlled by doing the same experiment with reversed solenoid field direction.

original proposal was to develop a compact, high-density fast calorimeter with good energy resolution at polar angles greater than 35° for the CLAS12 spectrometer [27], and occupy the radial space of ≈ 10 cm to fit inside the Central Solenoid. The tungsten powder technology has the benefits of compactness, homogeneity, simplicity, and favorable readout characteristics.

For the proposed elastic scattering experiment, the CEC would replace the current Central Neutron Detector, which occupies approximately the same radial space and polar angle range. The calorimeter will need to cover polar angles in a range of 40° to 130° , and the full 2π range in azimuth. From the original proposal there exists a prototype calorimeter that was designed, built, and cosmic-ray tested, and we plan to construct a CEC with parameters close the existing prototype calorimeter. The dimensions of the prototype's active volume are approximately length \times width \times height = $0.1 \times 0.1 \times 0.07$ m³ in volume and with 5,488 fibers (Bicron BCF-12) with 0.75 mm diameter, uniformly distributed inside the tungsten powder volume. These fibers make up 35% of the volume and the tungsten powder is filled into the remaining volume. The final density of the tungsten powder radiator is 12 g/cm³, or about 5% higher as compared with the density of bulk lead. The overall total density of the prototype active volume is ≈ 8.0 g/cm³. The estimated signal strength is about 75 photoelectrons per MeV. There is

the possibility of increasing the density of the radiator to $\approx 10.5 \text{ g/cm}^3$, which will lead to an increase of the detector absorption power. Also an additional increase can be obtained by simply decreasing sampling ratio, since having higher energy resolution is not a critical requirement. It has to be mentioned that due to the cylindrical shape of the CEC there will be no *side wall* effects.

2.2 Projected measurements

For the rate estimates and the kinematical coverage we have made a number of assumptions that are not overly stringent:

- i) Positron beam currents (unpolarized), $I_{e^+} \approx 60 \text{ nA}$;
- ii) Beam profile, $\sigma_x, \sigma_y < 0.4 \text{ mm}$;
- iii) Polarization not required, so phase space at the source can be optimized for yield and beam parameters;
- iv) Operate experiment with 5 cm liquid H_2 target and luminosity of $0.8 \times 10^{35} \text{ cm}^{-2} \cdot \text{sec}^{-1}$;
- v) Use the CLAS12 Central Detector for lepton (e^+/e^-) detection at $\Theta_l = 40^\circ - 125^\circ$;
- vi) Use CLAS12 Forward Detector for proton detection at $\Theta_p = 7^\circ - 35^\circ$.

We propose to take data at beam energies of 2.2, 3.3, 4.4 and 6.6 GeV, for 10 h, 50 h, 200 h and 1000 h respectively, split 1:1 in electron and positron running. The expected statistical errors, together with the expected effect size (phenomenological extraction from [19]) are shown in Fig. 7. The quality of the measured data will quantify hard two-photon-exchange over the whole region of precisely measured and to-be-measured cross section data, enabling a model-free extraction of the form factors from those. It will test if TPE can reconcile the form factor ratio data where the discrepancy is most significantly seen, and test, for the first time, GPD-based calculations.

2.3 Systematics of the comparison between electron and positron measurements

The main benefit to measure both lepton species in the same setup closely together in time is the cancellation of many systematics which would affect the result if data of a new positron scattering measurement is compared to existing electron scattering data. For example, one can put tighter limits on the change of detector efficiency and acceptance changes between the two measurements if they are close in time, or optimally, interleaved.

For the ratio, only relative effects between the species

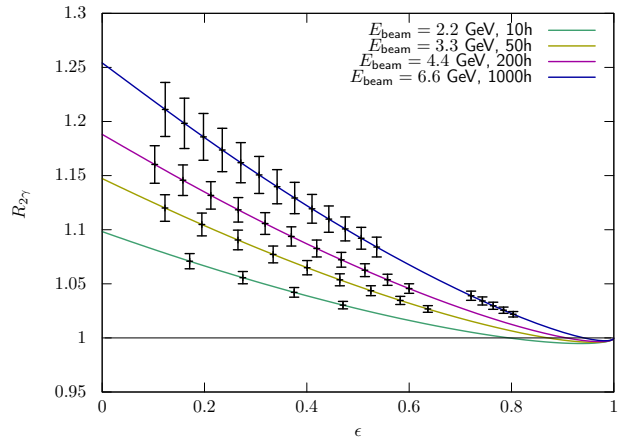


Fig. 7 Predicted effect size and estimated errors for the proposed measurement program at CLAS12. We assume bins of constant $\Delta Q^2 = 0.25 \text{ GeV}^2$. The prediction is based on [19].

types are relevant; the absolute luminosity, detector efficiency, etc. cancel. Compared to classic small acceptance spectrometers, even the requirements on the relative luminosity determination are somewhat relaxed, as all data points of one species share the same luminosity, that is, even without any knowledge of the relative normalization between species, the evolution of TPE as a function of ϵ for constant beam momenta could be extracted. To achieve then an absolute normalization of the ratio, the relative luminosity must be controlled.

The primary means of normalization for low current experiments in Hall B is the totally absorbing Faraday cup (FC) in the Hall B beam line. The absolute accuracy of the FC is better than 0.5% for currents of 5 nA or greater. The FC can be used in e^+/e^- beams with up to 500 W, which should not be a limitation for experiments in Hall B with CLAS12. The relative accuracy for the ratio of electrons to positrons should be at least as good as the absolute accuracy. The only known difference between electrons and positrons is the interaction of e^+ and e^- with the vacuum window at the entrance to the FC, which is a source of Møller scattering for electrons and a source of Bhabha scattering for positrons. The FC design contains a strong permanent magnet inside the vacuum volume and just after the window. This magnet is meant to trap (most of) the low-energy Møller electrons to avoid over-counting the electric charge. It will also trap (most of) the Bhabha scattered electrons from the positron beam to avoid under-counting (for positrons) the electric charge. However, there may be a remaining, likely small charge asymmetry for Møller and Bhabha scattered electrons in the response of the FC to the different charged beams. This effect will be studied in detail with a GEANT4 simulation. In any case, they relative efficiency of the

FC can be calibrated with a measurement of R at small scattering angles, i.e. $\epsilon \rightarrow 1$, where TPE effects become negligible. This calibration could be performed with the Forward Tagger Calorimeter which covers down to 2.5 degrees. The high counting rates make this a simple and fast calibration.

2.4 Radiative corrections

For an extraction of the hard part of the two-photon exchange, the measured raw ratio has to be corrected for radiative effects, including other charge-odd contributions. These include the soft two-photon exchange, but also the interference terms from radiation off the lepton and proton. Current radiative generators, for example ESEPP [28], or those from the A1 [19] and OLYMPUS experiments [26] allow us to include the radiative corrections as part of a full simulation, instead of a post-hoc correction factor.

The absolute size of the correction depend strongly on the cuts applied to select elastic reactions. Here, wider cuts lead to smaller corrections, however, not necessarily to smaller uncertainties, as the wider cuts accept kinematics further away from the elastic case captured in the theoretical calculations.

Figure 8 show an estimate of the radiative corrections (as corrections to a Born level calculation) for the four beam energies and both species. Here, selection cuts are chosen to accept missing energies (i.e., energies of the radiated photon) up to 20% of the outgoing lepton energy. Further, a 50 mrad-wide cut is applied on the lepton-angle vs. proton-angle correlation. For positrons, the charge-odd corrections reduce the size of the overall correction, however, the correction will have the same uncertainty as for the electron case, in which the charge-odd corrections have the same sign as the charge-even part.

2.5 Charge-averaged cross sections

In addition to a measurement of the ratio, the data set also allows a determination of the charge-averaged cross sections, similar to the recent results released by OLYMPUS [29], however with the added benefit of good absolute normalization. While the ratio is only sensitive to the charge-odd corrections, the charge-averaged cross sections cancel these, and are only sensitive to charge-even corrections. With the data set alone, Rosenbluth separations at several Q^2 up to about 7 (GeV/c)² will be possible and would allow a direct comparison with polarized measurements. Additionally, the data set will

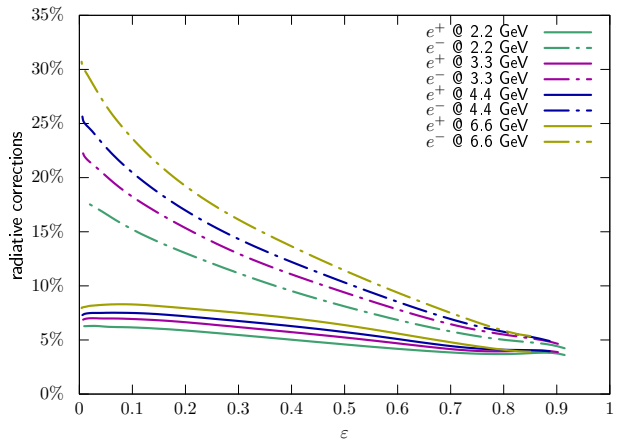


Fig. 8 Estimate of the radiative corrections for the four beam energies and both lepton charges. For positrons, the charge-odd corrections have an opposite sign from the charge-even corrections, reducing the overall size and drastically reducing the ϵ dependence.

be a helpful addition to the world data set and will reduce fit uncertainties in the covered Q^2 range.

3 Summary

Despite recent measurements of the e^+p/e^-p cross section ratio, the proton's form factor discrepancy has not been conclusively resolved, and new measurements at higher momentum transfer are needed. CLAS12, in combination with a positron beam at CEBAF, would be the definitive measurement of TPE over a wide and highly significant kinematic range. Only one major detector configuration change would be necessary to support such a measurement, the installation of the central electromagnetic calorimeter. In designing the JLab positron source, it will be crucial for this and several other experiments to keep to a minimum the time necessary to switch between electron and positron modes, in order to reduce systematic effects.

Acknowledgements This work was supported in part by the National Science Foundation grant number 2012114.

References

1. P.A.M. Guichon, M. Vanderhaeghen, Phys. Rev. Lett. **91** (2003) 142303.
2. C.E. Carlson, M. Vanderhaeghen, Ann. Rev. Nucl. Part. Sci. **57** (2007) 171.
3. J. Arrington, P.G. Blunden, W. Melnitchouk, Prog. Part. Nucl. Phys. **66** (2011) 782.
4. A.V. Afanasev *et al.* Prog. Part. Nucl. Phys. **95** (2017) 245.
5. L.W. Mo, Y.-S. Tsai, Rev. Mod. Phys. **41** (1969) 205.
6. L.C. Maximon, J.A. Tjon, Phys. Rev. C **62** (2000) 054320.

7. J. Litt *et al.* Phys. Lett. B **31** (1970) 40.
8. W. Bartel *et al.* Nucl. Phys. B **58** (1973) 429.
9. L. Andivahis *et al.* Phys. Rev. D **50** (1994) 5491.
10. R.C. Walker *et al.* Phys. Rev. D **49** (1994) 5671.
11. M.E. Christy *et al.* Phys. Rev. C **70** (2004) 015206.
12. I.A. Qattan *et al.* Phys. Rev. Lett. **94** (2005) 142301.
13. O. Gayou *et al.* Phys. Rev. C **64** (2001) 038202.
14. (Hall A Collaboration) V Punjabi *et al.* Phys. Rev. C **71** (2005) 055202; *err.* Phys. Rev. C **71** (2005) 069902.
15. M.K. Jones *et al.* Phys. Rev. C **74** (2006) 035201.
16. (Hall A Collaboration) A.J.R. Puckett *et al.* Phys. Rev. Lett. **104** (2010) 242301.
17. M. Paolone *et al.* Phys. Rev. Lett. **105** (2010) 072001.
18. (Hall A Collaboration) A.J.R. Puckett *et al.*, Phys. Rev. C **85** (2012) 045203.
19. J.C. Bernauer *et al.* Phys. Rev. C **90** (2014) 015206.
20. P.G. Blunden, W. Melnitchouk, Phys. Rev. C **95** (2017) 065209.
21. A.V. Afanasev *et al.* Phys. Rev. D **72** (2005) 013008.
22. I.A. Rachek *et al.* Phys. Rev. Lett. **114** (2015) 062005.
23. (CLAS Collaboration) M. Moteabbed *et al.* Phys. Rev. C **88** (2013) 025210.
24. (CLAS Collaboration) D. Adikaram *et al.* Phys. Rev. Lett. **114** (2015) 062003.
25. (CLAS Collaboration) D. Rimal *et al.* Phys. Rev. C **95** (2017) 065201.
26. (OLYMPUS Collaboration) B.S. Henderson *et al.* Phys. Rev. Lett. **118** (2017) 092501.
27. L.S. Cardman *et al.* White Paper: The Science Driving the 12 GeV Upgrade of CEBAF (2001).
28. A. V. Gramolin *et al.* J. Phys. G **41** (2014) 115001.
29. J. C. Bernauer *et al.* [arXiv:2008.05349 [nucl-ex]].